SoftwareX 23 (2023) 101407

Contents lists available at ScienceDirect

SoftwareX

journal homepage: www.elsevier.com/locate/softx

Original software publication

PROVER-M: A simple model to project the disposal of fine sediments

Jannek Gundlach *, Maximilian Behnke, Christian Jordan

Leibniz University Hannover, Ludwig Franzius Institute of Hydraulic, Estuarine and Coastal Engineering, Nienburger Straße 4, 30167 Hannover, Germany

ARTICLE INFO

Article history:
Received 19 January 2023
Received in revised form 5 May 2023
Accepted 8 May 2023

Keywords:
Sediment disposal
Dynamic plume
Near-field model
MATLAB

ABSTRACT

To improve sediment management strategies in coastal waters, the presented software, PROVER-M, uses a simple near-field model that projects the active distribution of fine sediments after a disposal of dredged material. PROVER-M aims to provide valuable input for far-field models, enabling them to more accurately simulate the disposal of fine sediments on a larger scale. Based on the input, PROVER-M calculates the dynamic plume behavior, including the convective descent of sediments and their dynamic collapse on the bottom. The result is a spatial distribution of disposed sediments through the water column and on the ground.

Code metadata

Current code version	v1.0
Permanent link to code/repository used for this code version	https://github.com/ElsevierSoftwareX/SOFTX-D-23-00051
Permanent link to Reproducible Capsule	https://github.com/JannekGundlach/PROVER-M
Legal Code License	GNU(GPL)
Code versioning system used	git
Software code languages, tools, and services used	MATLAB by MathWorks
Compilation requirements, operating environments & dependencies	MS Windows, MATLAB 2022a
If available, link to user manual—if formally published, include a reference to the publication in the reference list	none
Support email for questions	gundlach@lufi.uni-hannover.de

1. Motivation and significance

Sediment management (i.e., the dredging and disposal of sediment) plays a vital role in keeping waterways navigable and ensuring safe access to ports and harbors. To minimize the environmental impacts of dredged material, international agreements (e.g., [1]) provide guidelines for best practices. Focusing on Europe, the Marine Strategy Framework Directive (MSFD) [2] defines several descriptors that help to assess anthropogenic impacts on the marine environment and achieve good environmental status (GES). According to the MSFD, the disposal of dredged material may have adverse effects on the integrity of the seafloor (descriptor 6), contaminate the marine environment (descriptor 8), or induce underwater noise (descriptor 11). With growing maritime traffic and increasing vessel sizes [3], the rising demand for ship-based liquefied natural gas (LNG) and green hydrogen [4,5], and the intensified use of coastal areas [6,7], the amount of dredged material and the associated impacts on the environment are set to increase in the future. As shown in the case of the German Bight, sea-level rise (SLR) and the associated changes in tidal dynamics may also make estuaries more flood-dominant in the future (e.g., [8,9]), leading to enhanced landward-directed sediment transport. Hence, today and in the future, it is of the utmost importance that sediment management strategies be adopted to ensure that the dredging and disposal of sediment are handled in a sustainable manner. The localization of suitable disposal areas is particularly challenging, though process-based and complex numerical models may facilitate this task. However, widely applied numerical models from the field of coastal engineering (e.g., Delft3D [10]) are usually unable to accurately represent the dredging and disposal of fine sediments. Accordingly, near-field models are required to assess such complex small-scale processes. The results of the near-field models may later be transferred to far-field models (e.g., Delft3D), where the effects are then considered on a larger scale.

* Corresponding author.
E-mail address: gundlach@lufi.uni-hannover.de (Jannek Gundlach).

https://doi.org/10.1016/j.softx.2023.101407

To address this need, the near-field model PROVER-M was developed to represent the driving mechanisms for the disposal of fine sediments in a detailed manner. Given that the PROVER-M code was published under an open-source license, it may be applied by scientists and stakeholders from the public and private sectors who wish to project the effects of fine sediment disposal. In addition to being open-source and freely available, the model covers all relevant processes and is simple to use; it differs from existing near-field models in its approach to the disposal of fine sediments. Indeed, other models are either poorly accessible (e.g., Jet3D [11–13]), do not cover the whole disposal process (e.g., the analytical Krishnappen model [14]), are poorly maintained (e.g., Short Term Fate (STFATE) [15–19]), or lack relevant processes for fine sediment disposal (e.g., Barged Sediment Disposal Model (BSDM) [20,21]). Even though the recently published BSDM (version 2.0) is more detailed in its consideration of the shape of the descending cloud compared to PROVER-M, it is more applicable for sand because it calculates a large amount of settling, over-predicts the final radius of the sediment cloud while under-predicting its height, and neglects the important process of sediment being brought into passive suspension. Although an MS-DOS version of STFATE exists, it is a black box in regard to some parameter settings, and it likely under-predicts the cloud width at the end of the dynamic collapse. The PROVER-M model addresses these limitations by adapting existing knowledge and model approaches, simplifying processes where possible, and making the code as accessible as possible for further crowd-sourced development.

2. Sediment disposal

Fine sediments mixed with water behave like dense fluid when released from a dredging vessel. The high water content and fine particle size allow the assumption of a homogeneous sediment-water mixture that behaves like a defined cloud when released into water. The behavior after an instantaneous disposal is often divided into three phases: (i) convective descent, (ii) dynamic collapse, and (iii) passive diffusion [15,22,23]. During the convective descent, negative buoyancy leads to a downward motion of the well-defined cloud. Rahimipour and Wilkinson [24] further divided the descent into an initial acceleration phase, a self-preserving phase, and a dispersive phase, including the analogy to a thermal. Between the self-preserving and the dispersive phases, the cloud grows due to entrainment of ambient water. Additionally, entrainment and turbulent shear stresses on the cloud's interface cause parts of the sediment cloud to separate, which then remain in the water for passive transport [25,26]. This process is called sediment stripping. The dynamic collapse starts upon impact with the ground, including the radial horizontal spreading on the bottom based on the conservation of motion. While the radial spreading prevails over ambient currents, the second phase continues with coarser material settling. Passive diffusion starts as soon as ambient currents become dominant, at which point the material is diffused by the local currents and flow fields.

3. Model description

The PROVER-M model is based on mathematical approximations that describe the fluid–fluid interaction during the convective descent [15,16,27,28] and the spreading of a density current after impact on the ground based on the conservation of energy [18]. Here, the assumption is that the disposed sediment cloud is a homogeneously mixed unit that descends as one body, which is approximated as the lower half of a sphere. After impact, the sediment cloud remains as the upper half of an ellipsoid, where the horizontal extent grows while the vertical height decreases due to radial spreading. This concept has previously been applied by [15,16,18] and the model STFATE. Further simplifications are introduced in the description of the ambient conditions, where a constant flow field and a flat bottom are introduced.

3.1. Convective descent

The behavior of the instantaneously released sediment-water mixture is described by the conservation of mass (Eq. (1)), momentum (Eq. (2)), buoyancy (Eq. (3)), vorticity (Eq. (4)), and the amount of solids (Eq. (5)). Following Koh and Chang [15], mathematical formulations for the first phase in the context of a one-dimensional mathematical framework read as follows:

Conservation of mass. The conservation of mass (volume and density of the cloud) is determined by the entrained fluid as a source and the detached sediments as a sink:

$$dV_{Cloud}\frac{\rho}{dt} = E\rho_a - \sum_i S_i\rho_i \tag{1}$$

where E is the entrainment rate (Eq. (6)), ρ_a is the ambient density, while S_i and ρ_i are the stripped sediment volume of a selected sediment fraction i and its specific density, respectively.

Conservation of momentum. By balancing the buoyancy force, drag force, stripped material, and entrained fluid, the conservation of momentum is achieved:

$$\frac{dM}{dt} = Fj - D + E\rho_a u_a - \sum_i S_i\rho_i \tag{2}$$

with F being the buoyancy force with its vector j, D being the drag force, and u_a being the ambient velocity for the specified direction. Regarding further insight into the buoyancy and drag force, the reader is referred to Brandsma and Divoky [16].

Conservation of buoyancy. The clouds buoyancy is balanced by considering the change in the density differences between the cloud and the ambient fluid due to entrainment and stripping:

$$\frac{dB}{dt} = E\left(\rho_a(0) - \rho_a\right) - \sum_i S_i\left(\rho_a(0) - \rho_i\right) \tag{3}$$

including $\rho_a(0)$ as the initial (surface) ambient density.

Conservation of vorticity. The vorticity of the cloud is reduced by the relative density difference of the ambient fluid:

$$\frac{dK}{dt} = -\frac{Ca^2 g}{\rho_a(0)}\frac{d\rho_a}{dz} \tag{4}$$

with C as a constant for vorticity dissipation, a as the vertical extent of the cloud, g as the gravity constant, and $\frac{d\rho_a}{dz}$ as the density gradient of the ambient fluid.

Conservation of solids. In the conservation of solids, all material losses due to stripping lead directly to a decrease in the solids content in the cloud:

$$\frac{dP_i}{dt} = -S_i \tag{5}$$

Entrainment. A decisive part of the conservation equations is the entrainment, which is calculated by the lateral cloud surface and the absolute difference between the cloud motion and the ambient velocity:

$$E = 2\pi a^2 \alpha \left|U - U_a\right| \tag{6}$$

with U being the cloud motion, U_a being the ambient current, and α being the entrainment coefficient. The entrainment coefficient is an important calibration parameter in STFATE [29] and can be determined based on the moisture content [18,30]. In PROVER-M, the entrainment coefficient is used as a user-defined calibration parameter and should be treated carefully (see 3.4).

Sediment stripping. The stripping of sediment, where only fine sediments are considered, is dependent upon the entrainment of ambient fluid. Thus, it is calculated according to the amount of entrainment and an input factor Ψ_{strip} defined as follows:

$$V_{strip} = \Psi_{strip} E = \Psi_{strip} 2\pi a^2 |U - U_a| \tag{7}$$

In literature, a fraction of $2 - 5\%$ of the disposed sediment is reported to be stripped during disposal [18,25], which can then be used to estimate proper values for Ψ_{strip} during the calibration process.

3.2. Dynamic collapse

The radial spreading and vertical decline of the sediment cloud on the ground are described by the conservation of energy. The initial potential energy (Eq. (10)) and the initial kinetic energy (Eq. (11)) are estimated based on the last convective descent state and applied to estimate the spreading in the dimensions x (Eq. (12)), y (Eq. (13)), and z (Eq. (14)). The concept of energy conservation balances the change in potential energy and losses to determine the kinetic energy (Eq. (8)). The mathematical discretization has been derived by [16,18].

Conservation of energy. The change in kinetic energy in each time step is determined by the change in potential energy reduced by drag, friction, and turbulent losses, considered as work done [18]. Thus, work will reduce the kinetic energy, while the reduction of potential energy will increase the kinetic energy:

$$\Delta E_{pot} = \sum Work - \Delta E_{kin} \tag{8}$$

Change in potential energy. Changes in potential energy are based on the reduction in the distance of the cloud's center of gravity to the ground and mass losses due to settling and entrainment:

$$\Delta E_{pot} = \frac{3}{8} \left(\Delta\rho_t - \Delta\rho_{t+1}\right) g \left(V_t - V_{t+1}\right) \left(a_t - a_{t+1}\right) \tag{9}$$

with the density difference between the cloud and the ambient fluid $\Delta\rho$.

Initial potential and kinetic energy. The initial potential energy at the end of the convective descent is calculated based on the distance of the cloud's center of gravity to the ground and its mass:

$$E_{pot} = 0.25 \Delta\rho g r^3 a \tag{10}$$

The initial kinetic energy is based on the clouds motion and mass at the end of the convective descent:

$$E_{kin} = \frac{1}{3} \rho\pi r^3 |U|^2 \tag{11}$$

Cloud spreading in x-, y-, z-direction. The spreading of the cloud on the ground is divided into the horizontal (x, y) and vertical directions (z). It is based on the growth of the cloud due to entrainment and flattening of the cloud due to the kinetic energy redirection along the ground. By being approximated by the upper half of an ellipsoid and taking into account the ratios of the cloud dimensions, the spreading in x-direction $\frac{\Delta b}{\Delta t}$ can be estimated:

$$\left(1 + \frac{b^2}{c^2} + \frac{a^2}{b^2} + \frac{2a^2}{c^2} + \frac{a^2 b^2}{c^4}\right) \left[\frac{\Delta b}{\Delta t}\right]^2 - \frac{2Q_e}{V\left(\frac{1}{b} + \frac{b}{c^2}\right)} \left[\frac{\Delta b}{\Delta t}\right]$$

$$= \frac{10 E_{kin}}{\rho V} - a^2 \frac{Q_e^2}{V^2} \tag{12}$$

with Q_e being the entrainment rate, V being the cloud volume, and E_{kin} being the total kinetic energy. The spreading in y-direction $\frac{\Delta c}{\Delta t}$ is solely dependent on the ratio between the x- and y-dimension of the cloud and the spreading in x-direction, as the ratio of x and y is kept constant in the horizontal plane:

$$\left[\frac{\Delta c}{\Delta t}\right] = \frac{b}{c} \left[\frac{\Delta b}{\Delta t}\right] \tag{13}$$

The reduction of the height of the cloud in z-direction $\frac{\Delta a}{\Delta t}$ is based on the conservation of the cloud volume, including the entrainment rate and the relation of the cloud geometry to the horizontal spreading:

$$\left[\frac{\Delta a}{\Delta t}\right] = a \left(\frac{Q_e}{V} - \frac{\left[\frac{\Delta b}{\Delta t}\right]}{b} - \frac{\left[\frac{\Delta c}{\Delta t}\right]}{c}\right) \tag{14}$$

Sediment settling. Based on Partheniades–Krone's deposition equation [31,32], the deposition flux D in PROVER-M is calculated as follows:

$$D = w_s c_b \Gamma \tag{15}$$

where w_s is the fall velocity, c_b is the near-bed sediment concentration, and Γ is a dimensionless reduction factor defined by the following:

$$\Gamma = \begin{cases} 1 - \frac{\tau_c}{\tau_{cr,d}} & when \quad \delta < 0 \\ \delta & when \quad 0 < \delta < 1 \end{cases} \tag{16}$$

where τ_c is the current-induced shear-stress, $\tau_{cr,d}$ is a user-defined critical shear-stress for deposition, and δ is a user-defined deposition efficiency. If the value for δ is chosen to be smaller than 0, the reduction factor is determined based on the defined critical shear-stress for deposition.

3.3. Flow chart

The model code can be divided into five elements: (i) the user input, (ii) the main program code, (iii) the phase criteria, (iv) the numerical solver, and (v) the two phase functions. Fig. 1 presents the general structure of the simulation process. Input defined via the graphical user interface (GUI) is transferred to the main program code, where the bookkeeping of the calculation parameters occurs.

An iteration over time for the phase of convective descent is entered, in which initial variables for cloud and ambient conditions are determined during the first run. Depending on whether the bottom is encountered, calculations continue in the phase of convective descent or proceed to the phase of dynamic collapse. If the cloud has not encountered the bottom, the numerical solver is entered with the current cloud and ambient characteristics. Parameter gradients are approximated using the Runge–Kutta 4th-order method. After that, all required variables are updated using the conservation equations presented in Section 3.1 (Eqs. (1)–(5)). Here, the value of the previous iteration is added to the gradient of the current iteration. Then newly calculated parameters are passed to the main program code, where the amount of stripped material is determined, and cloud and ambient characteristics are stored in an output file. The iteration then continues until the cloud encounters the bottom. Following the transition to the phase of dynamic collapse, the described program structure remains the same. However, now the numerical solver updates the parameters using the energy concept of Section 3.2 (Eqs. (8), (12), (13), (14)), while the settled material is determined instead of the stripped material. Once ambient currents prevail over the radial cloud spreading velocity, the exit criteria is met and the program code is terminated.

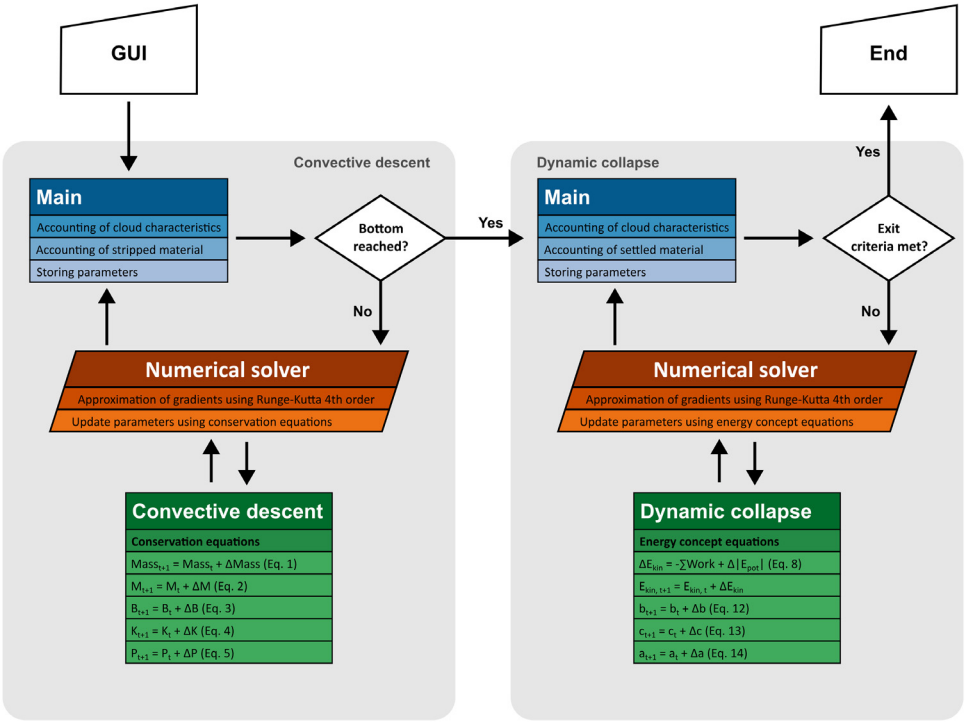

Fig. 1. PROVER-M flow-chart: The convective descent (left) and dynamic collapse (right) are iterated over time, comprising parameter bookkeeping (main, blue), parameter gradients per time-step (numerical solver, brown), and phase related functions (conservation and energy concept equations, green). Initialization is done via the GUI, while model criteria (diamonds) determine the transition to the dynamic collapse (bottom is encountered), and termination of the program (ambient currents prevail over radial spreading).

3.4. Selection of parameters

The model input is categorized using ambient and hopper settings and model coefficients. The former describe the physical parameters of the environment and disposal configuration, while the latter represent the empirical parameters of the fluid–fluid interaction. Ranges of the physical parameters are chosen for expected values in open-water disposal processes, while the orders of magnitudes for empirical coefficients are based on the literature sources mentioned below and are calibrated for the field data used in the illustrative example (see Section 4).

Default values for the entrainment, drag, mass, friction, and stripping coefficients are based on [29,30], and [18]. Furthermore, a sediment loss of 2% and 5% (for depths until 30 m) during a disposal process was chosen based on the findings of [18,26,33,34], and [25].

Users of PROVER-M are advised to consult the source code repository (see Code metadata Table) for further information regarding the model input. Parameter limits within the GUI should prevent implausible model behavior. When applying PROVER-M to a specific case, model coefficients should be chosen with care and calibrated and validated wherever possible.

4. Illustrative example

The PROVER-M model can be applied to various disposal simulations. The dynamic behavior of a disposed cloud, which was measured by HR Wallingford [35] in Tees Bay (England) (see Fig. 2), is used below as an illustrative example. For the simulation, an average disposal event with an ambient velocity in the range of 0.2 m/s to 0.4 m/s is taken. An average local water depth of 27 m with a flat ground is present at the disposal site. The used hopper dredger had a capacity of 1550 m^3, and the dredged material had an average density of 1150 kg/m^3 with a mean silt content of 50%. Entering the input in the GUI and running the model with adjusted drag coefficients only results in a symmetrical, elliptical cloud with a diameter of 166 m and a center height of 1.4 m (see Table 1). These dimensions reflect the end of the dynamic/active cloud behavior and can serve as an input for further far-field simulations. During the descent, approximately 6.5% of the material is stripped and remains in the water column. To illustrate the vertical motion and distribution of sediments, the sediment concentration in the horizontal plain integrated over time is given in Fig. 3. The high concentrations in darker red denote the vertical axis of the cloud, while the lighter red-orange color indicates the stripped material. The descent of the cloud until the bottom is encountered can be seen from 0 s to 8.5 s on the left side of Fig. 3, with entrainment of ambient water leading to an increase in the radius from 9 m to 12 m. After that, during the collapse, the cloud decreases non-linearly in the vertical axis due to the radial spreading until a height of 1.4 m is reached after 100 s, as shown on the right side of Fig. 3.

During the field test at Tees Bay, the spreading velocity of the cloud on the ground during the second phase was reported at a distance of 50 m, 75 m, 135 m, and 155 m, from the disposal location. These velocities are compared to the simulated horizontal spreading velocity in Fig. 4a, providing valuable insight into the physical properties of the cloud. The simulated spreading velocity can be seen until a cloud radius of 83 m only, at which point the end of the second phase is reached, and further spreading becomes part of the passive diffusion in a far-field model. However, the decaying spreading velocity matches the measured values well at 50 m and 75 m.

By comparing the results of PROVER-M to STFATE and BSDM for the HR Wallingford study, the strengths of the PROVER-M model are highlighted in Fig. 4b and Table 1. Wherever possible, the same input parameters were chosen across all models (supplementary material). While the simulation results for the three models are relatively similar for the convective descent phase (dotted lines in Fig. 4b and Table 1), the development of the cloud

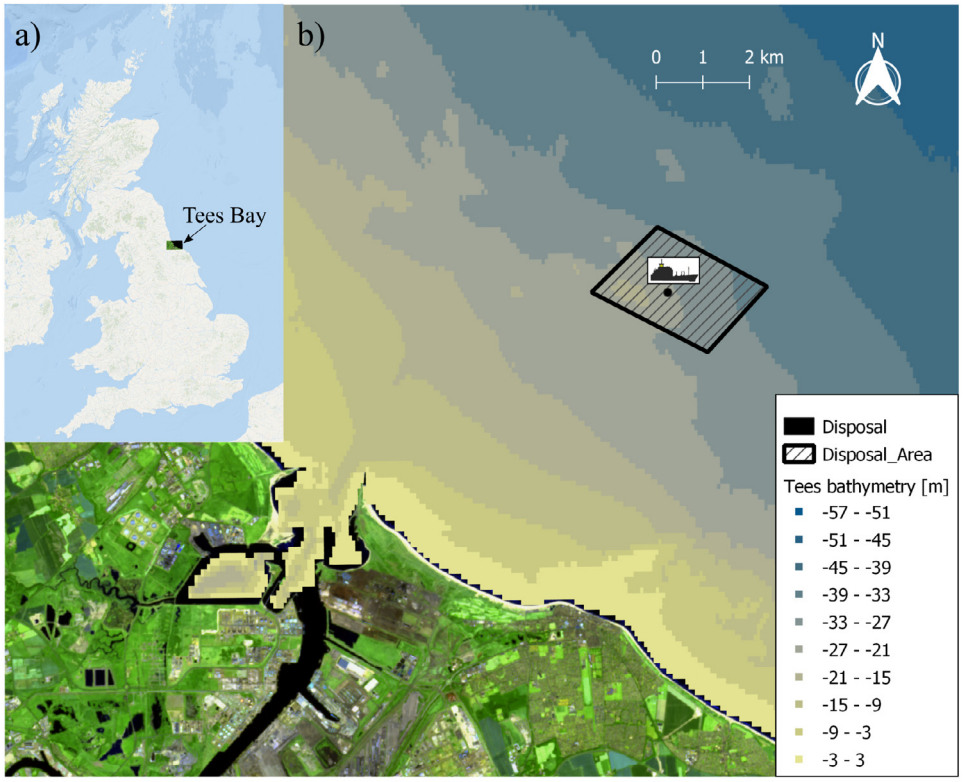

Fig. 2. Top view of Tees Bay with the indicated disposal area mentioned in [35]. Part a) shows the location of Tees Bay, while b) presents the disposal area of the illustrative case at Tees Bay. Satellite data are taken from Sentinel 2, EO Browser, and bathymetry data originate from the European Marine Observation and Data Network (EMODnet).

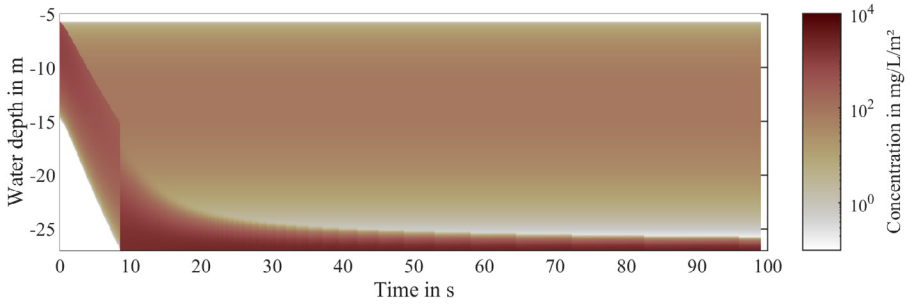

Fig. 3. PROVER-M simulation results of the sediment concentration in the vertical over time for the HR Wallingford study [35], with high concentrations representing the cloud and medium concentrations representing stripped material.

width over time during the dynamic collapse reveals considerable differences. Whereas the STFATE simulation reaches the end of the dynamic collapse after 32 s with a diameter of 117 m, the BSDM simulation terminates after 138 s and 443.4 m. In contrast, PROVER-M reaches the end of the dynamic collapse after 100 s with a cloud width of 166 m. Although STFATE and PROVER-M both apply the energy concept to calculate the dynamic collapse, the development of the cloud width over time differs significantly. The authors assume that this arises from the applied conversion of potential energy into kinetic energy (Eq. (8)). When the loss of potential energy in PROVER-M is considered a sink for kinetic energy, the model results resemble those of STFATE. However, it seems to be physically more correct to consider the reduction of potential energy to be a source of kinetic energy. The BSDM results suggest the rapid and strong growth of the cloud width, which is not consistent with the observations of [35]. In addition, BSDM computes a significantly larger cloud width (>250%) and amount of settled material compared to STFATE or PROVER-M, while the cloud height is two orders of magnitude smaller (see Table 1). This might be based on the development of BSDM for sandy material, although a mean sediment diameter is part of the model input. Furthermore, BSDM does not consider ambient currents or calculate sediment stripping. Of the considered models, PROVER-M is best suited to accurately model and project the values measured by [35].

5. Impact

A simplified version of the model was implemented into the dredging- and dumping-module DredgeSim of the process-based sediment transport model UnTRIM-SediMorph [36] and is applied at the Federal Waterways Engineering and Research Institute (BAW). The PROVER-M model contributes to the field of sediment management by providing an easy tool that can be applied to project the distribution of disposed fine sediments in estuarine and coastal environments. Model-based projections of the effect of fine sediment disposals, where a low resolution and a simple mass transfer to the bottom are not sufficient, will benefit from

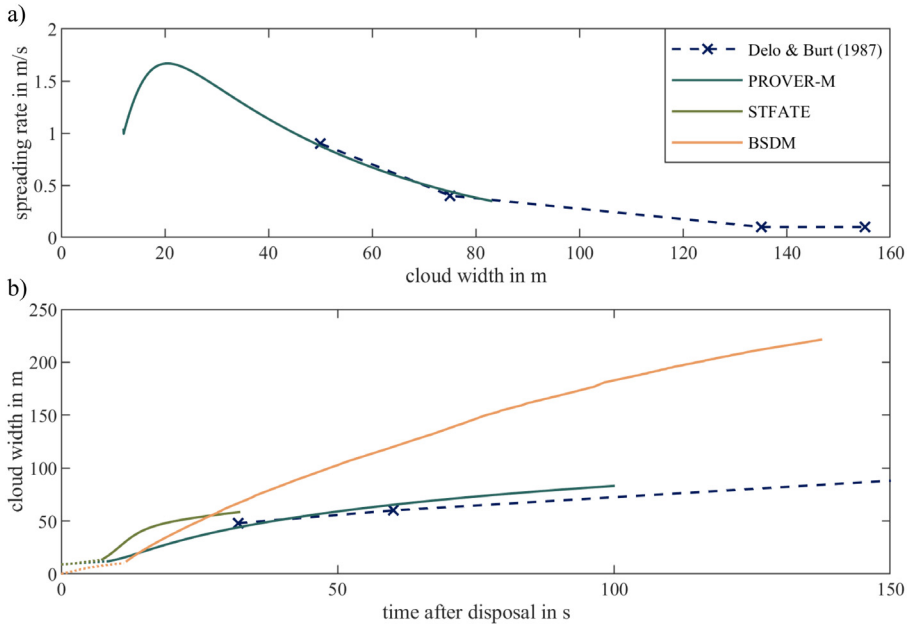

Fig. 4. Comparison of PROVER-M against field measurements, STFATE, and BSDM. a) Horizontal spreading velocity of the cloud on the ground based on field measurements by HR Wallingford [35] and PROVER-M. b) Comparison of cloud widths (center to front) over time for the PROVER-M, STFATE, and BSDM models. Dotted lines indicate the convective descent, while solid lines denote the dynamic collapse phase (the ends of the lines correspond to each model's internal end of the dynamic collapse).

Table 1
Model results of PROVER-M, STFATE, and BSDM for the convective descent and dynamic collapse based on the conditions described in the HR Wallingford study [35]. Models are compared by time, radius, and stripped material at the end of the convective descent and time, diameter, height, and settled material at the end of the dynamic collapse.

Model	Convective descent			Dynamic collapse			
	t [s]	r [m]	strip [%]	t [s]	d [m]	h [m]	setl. [%]
PROVER-M	8.4	12	6.5	100	166.4	1.4	0.1
STFATE	7.2	13.2	1.2	32	117.0	1.7	5.1
BSDM	11.3	9.9	–	138	443.3	0.03	98.8

using PROVER-M. In addition, the model may provide valuable input for detailed environmental and navigational assessments. Here, a higher degree of detail enables stakeholders to be more accurate in projections of the sediment distribution. Potentially, this can lead to locally more accurate/sustainable disposal strategies (e.g., when to dispose which material at which disposal site), which in turn can be ecologically and economically beneficial. Given that space in intensively managed estuaries and coastal areas is becoming scarce and the accurate prediction of human-induced (disposal) processes is becoming more important, PROVER-M has the potential to be attractive for local port authorities, federal agencies, private companies, and scientists in regard to sediment management and sediment disposal constraints. Furthermore, the accessibility and simple structure of the model enable it to open opportunities to adapt or further develop PROVER-M. For example, an integration into existing far-field models or an extension of further details, such as slope effects, can easily be made. In addition, the ability to fine-tune PROVER-M, through input parameters and the open-source code, allows particularly case-specific model setups.

6. Conclusions

Based on conservation equations and the user-defined input, the PROVER-M model simulates the near-field dynamic behavior of fine sediments after disposal. The model can be used to project the vertical and horizontal distribution of sediment clouds after disposal. Moreover, in contrast to existing near-field models, PROVER-M is written for fine sediments, covers the important processes in a simple and comprehensible way, and is open source. The fully functional source code of the model is written in MATLAB and comes with a GUI that combines the functions of the two phases, the numerical solver, and the main bookkeeping. Simulating the important near-field processes, it enables a more accurate representation of disposals than conventional far-field models. The use of PROVER-M can be beneficial for all stakeholders dealing with sediment management and disposals.

CRediT authorship contribution statement

Jannek Gundlach: Conceptualization, Methodology, Software, Validation, Investigation, Data curation, Writing – original draft, Writing – review & editing, Visualization, Funding acquisition. **Maximilian Behnke:** Software, Data curation, Writing – original draft, Writing – review & editing, Visualization. **Christian Jordan:** Writing – original draft, Writing – review & editing.

Declaration of competing interest

The authors declare that they have no known competing financial interests or personal relationships that could have appeared to influence the work reported in this paper.

Data availability

Input data is provided with the source code and supplementary material.

Acknowledgments

The development of the PROVER-M model was funded by the Federal Waterways Engineering and Research Institute (BAW), Germany in Hamburg (2018–2021). The authors would like to acknowledge the importance of the technical discussions we had with Anna Zorndt, Holger Weilbeer, and Benjamin Fricke from BAW Hamburg during the development of this project. Further thanks go to our colleagues at the Ludwig Franzius Institute for their support during the development and writing of the model and this paper. The authors also appreciate the work done by Marlena Gundlach for the graphic design of the PROVER logo. Colormaps applied in the illustrative example section are based on scientific colormaps [37,38]. The publication of this article was funded by the Open Access Fund of Leibniz Universität Hannover.

Appendix A. Supplementary data

Supplementary material related to this article can be found online at https://doi.org/10.1016/j.softx.2023.101407.

References

[1] OSPAR Commission. OSPAR guidelines for the management of dredged material at sea (agreement 2014-06). 2014, https://www.ospar.org/documents?d=34060, [Accessed 27 April 2023].

[2] European Commission. Directive 2008/56/EC of the European Parliament and of the Council of 17 June 2008 establishing a framework for community action in the field of marine environmental policy (Marine Strategy Framework Directive). Off J Eur Union 2008;L 164:19–40, https://eur-lex.europa.eu/legal-content/EN/TXT/?uri=celex%3A32008L0056, [Accessed 27 April 2023].

[3] Garrido J, Saurí S, Marrero Á, Gül Ü, Rúa C. Predicting the future capacity and dimensions of container ships. Transp Res Rec 2020;2674(9):177–90. http://dx.doi.org/10.1177/0361198120927395.

[4] International Energy Agency. The future of hydrogen: Seizing today's opportunites. Paris, France: International Energy Agency; 2019, https://www.iea.org/reports/the-future-of-hydrogen, [Accessed 27 April 2023].

[5] Johnston C, Ali Khan MH, Amal R, Daiyan R, MacGill I. Shipping the sunshine: An open-source model for costing renewable hydrogen transport from Australia. Int J Hydrogen Energy 2022;47(47):20362–77. http://dx.doi.org/10.1016/j.ijhydene.2022.04.156.

[6] Nicholls RJ. Coastal flooding and wetland loss in the 21st century: Changes under the SRES climate and socio-economic scenarios. Glob Environ Change 2004;14(1):69–86. http://dx.doi.org/10.1016/j.gloenvcha.2003.10.007.

[7] Neumann B, Vafeidis AT, Zimmermann J, Nicholls RJ. Future Coastal population growth and exposure to sea-level rise and coastal flooding - A global assessment. PloS ONE 2015;10(3):e0118571. http://dx.doi.org/10.1371/journal.pone.0118571.

[8] Wachler B, Seiffert R, Rasquin C, Kösters F. Tidal response to sea level rise and bathymetric changes in the German Wadden Sea. Ocean Dynam 2020;70:1033–52. http://dx.doi.org/10.1007/s10236-020-01383-3.

[9] Jordan C, Visscher J, Schlurmann T. Projected responses of tidal dynamics in the North Sea to sea-level rise and morphological changes in the Wadden Sea. Front Mar Sci 2021;8:685758. http://dx.doi.org/10.3389/fmars.2021.685758.

[10] Lesser GR, Roelvink JA, van Kester JATM, Stelling GS. Development and validation of a three-dimensional morphological model. Coast Eng 2004;51(8–9):883–915. http://dx.doi.org/10.1016/j.coastaleng.2004.07.014.

[11] Delvigne GAL. Gedrag baggerspecie bij storten: Verslag rekenwerk. Delft, Netherlands: Delft Hydraulics Laboratory; 1979, https://repository.tudelft.nl/islandora/object/uuid:42563e37-aa60-49d6-94bf-3d38c8afabc4, [Accessed 27 April 2023].

[12] Delvigne GAL, Sweeney CE. Natural dispersion of oil. Oil Chem Pollut 1988;4(4):281–310. http://dx.doi.org/10.1016/S0269-8579(88)80003-0.

[13] Aarninkhof S, Luijendijk A. Safe disposal of dredged material in an environmentally sensitive environment. Port Technol Int 2010;47:39–45, https://www.porttechnology.org/technical-papers/safe_disposal_of_dredged_material_in_an_environmentally_sensitive_envi/, [Accessed 27 April 2023].

[14] Krishnappan BG. Dispersion of dredged spoil when dumped as a slug in deep water: The Krishnappan model. In: Proceedings of workshop on fate models to predict the dispersion of drilling fluids and cuttings from offshore oil platforms. 1983, p. 1–23, Santa Barbara, California, USA.

[15] Koh RCY, Chang YC. Mathematical model for barged ocean disposal of wastes. Washington, D.C., USA: Office of Research and Development, U.S. Environmental Protection Agency; 1973, https://purl.fdlp.gov/GPO/gpo84296, [Accessed 27 April 2023].

[16] Brandsma MG, Divoky DJ. Development of models for prediction of short-term fate of dredged material discharged in the estuarine environment. Pasadena, California, USA: Tetra Tech, Incorporated; 1976, https://usace.contentdm.oclc.org/digital/collection/p266001coll1/id/5455/, [Accessed 27 April 2023].

[17] Johnson BH. User's guide for models of dredged material disposal in open water. Vicksburg, Mississippi, USA: U.S. Army Engineer Waterways Experiment Station; 1990, https://erdc-library.erdc.dren.mil/jspui/handle/11681/4652, [Accessed 27 April 2023].

[18] Johnson BH, Fong MT. Development and verification of numerical models for predicting the initial fate of dredged material disposed in open water. Report 2. Theoretical developments and verification results. Vicksburg, Mississippi, USA: U.S. Army Engineer Waterways Experiment Station; 1995, https://apps.dtic.mil/sti/citations/ADA292918, [Accessed 27 April 2023].

[19] Schroeder PR, Palermo MR, Myers TE, Lloyd CM. The automated dredging and disposal alternatives modeling system (ADDAMS). Vicksburg, Mississippi, USA: U.S. Army Engineer Research and Development Center; 2004, https://apps.dtic.mil/sti/citations/ADA430416, [Accessed 27 April 2023].

[20] Er JW, Law AWK, Adams EE, Zhao B. Open-water disposal of barged sediments. J Waterway Port Coast Ocean Eng 2016;142(5):04016006. http://dx.doi.org/10.1061/(ASCE)WW.1943-5460.0000341.

[21] Er JW, Law AW-K, Adams EE. Spreading and deposition of turbidity currents: Application to open-water sediment disposal. J Waterw Port Coast Ocean Eng 2020;146(3):04020002. http://dx.doi.org/10.1061/(ASCE)WW.1943-5460.0000556.

[22] Clark BD, Rittall WF, Baumgartner DJ, Byram KV. The barged ocean disposal of wastes: A review of current practice and methods of evaluation. Corvallis, Oregon, USA: U.S. Environmental Protection Agency, Pacific Northwest Water Laboratory; 1971, https://nepis.epa.gov/Exe/ZyPURL.cgi?Dockey=9101RTKH.TXT, [Accessed 27 April 2023].

[23] Delo E, Ockenden MC, Burt TN. Dispersal of dredged material - mathematical model of plume. Wallingford, England: Hydraulics Research Wallingford; 1987, https://eprints.hrwallingford.com/161/, [Accessed 27 April 2023].

[24] Rahimipour H, Wilkinson D. Dynamic behavior of particle clouds. In: Proceedings of 11th Australasian fluid mechanics conference. Hobart, Australia; 1992, p. 743–6.

[25] Truitt CL. Dredged material behavior during open-water disposal. J Coast Res 1988;4(3):489–97, https://journals.flvc.org/jcr/article/view/77784, [Accessed 27 April 2023].

[26] Lai ACH, Adams EE, Law AW-K. Mass loss to the trailing stem of a sediment cloud. J Hydraul Eng 2018;144(4):06018003. http://dx.doi.org/10.1061/(ASCE)HY.1943-7900.0001417.

[27] Scorer RS. Experiments on convection of isolated masses of buoyant fluid. J Fluid Mech 1957;2(6):583–94. http://dx.doi.org/10.1017/S0022112057000397.

[28] Abraham G. The flow of round buoyant jets issuing vertically into ambient fluid flowing in a horizontal direction. In: Proceedings of 5th international water pollution research conference. San Francisco, California, USA; 1970, p. 7.

[29] Johnson BH, Holliday BW. Evaluation and calibration of the Tetra Tech dredged material disposal models based on field data. U.S. Army Engineer Waterways Experiment Station; 1978, https://apps.dtic.mil/sti/citations/ADA059991, [Accessed 27 April 2023].

[30] Bowers GW, Goldenblatt MK. Calibration of a predictive model for instantaneously discharged dedged material. Corvallis, Oregon, USA: U.S. Environmental Protection Agency, Environmental Research Laboratory; 1978, https://nepis.epa.gov/Exe/ZyPURL.cgi?Dockey=9100T51P.TXT, [Accessed 27 April 2023].

[31] Krone RB. Flume studies of the transport of sediment in estuaries shoaling processes. Berkeley, California, USA: Hydraulic Engineering Lab-

oratory and Sanitary Engineering Research Laboratory, University of California; 1962.
[32] Partheniades E. Erosion and deposition of cohesive soils. J Hydraul Div 1965;91(1):105–39. http://dx.doi.org/10.1061/JYCEAJ.0001165.
[33] Ruggaber GJ. Dynamics of particle clouds related to open-water sediment disposal (Ph.D. thesis), Cambridge, Massachusetts, USA: Massachusetts Institute of Technology; 2000, https://dspace.mit.edu/handle/1721.1/9009, [Accessed 27 April 2023].
[34] Gensheimer RJ, Adams EE, Law AWK. Dynamics of particle clouds in ambient currents with application to open-water sediment disposal. J Hydraul Eng 2013;139(2):114–23. http://dx.doi.org/10.1061/(ASCE)HY.1943-7900.0000659.
[35] Delo E, Burt TN. Dispersal of dredged material - Tees field study September 1986. Wallingford, England: Hydraulics Research Wallingford; 1987, https://eprints.hrwallingford.com/172/, [Accessed 27 April 2023].
[36] Casulli V, Walters RA. An unstructured grid, three-dimensional model based on the shallow water equations. Int J Numer Methods Fluids 2000;32(3):331–48. http://dx.doi.org/10.1002/(SICI)1097-0363(20000215)32:3<331::AID-FLD941>3.0.CO;2-C.
[37] Crameri F, Shephard GE, Heron PJ. The misuse of colour in science communication. Nat Commun 2020;11:5444. http://dx.doi.org/10.1038/s41467-020-19160-7.
[38] Crameri F. Scientific colour maps. 2021, http://dx.doi.org/10.5281/ZENODO.1243862, Dataset on Zenodo.